NEOPLASIA
www.neoplasia.com

Volume 17 Number 12 December 2015 pp. 882–893 882

Polyploidy Formation in Doxorubicin-Treated Cancer Cells Can Favor Escape from Senescence [1]

Grazyna Mosieniak[2], Malgorzata A. Sliwinska[2], Olga Alster, Anna Strzeszewska, Piotr Sunderland, Malgorzata Piechota, Halina Was and Ewa Sikora

Laboratory of Molecular Bases of Aging, Nencki Institute of Experimental Biology, Polish Academy of Sciences, Warsaw, 02-093 Poland

Abstract

Cancer cells can undergo stress-induced premature senescence, which is considered to be a desirable outcome of anticancer treatment. However, the escape from senescence and cancer cell repopulation give rise to some doubts concerning the effectiveness of the senescence-induced anticancer therapy. Similarly, it is postulated that polyploidization of cancer cells is connected with disease relapse. We postulate that cancer cell polyploidization associated with senescence is the culprit of atypical cell divisions leading to cancer cell regrowth. Accordingly, we aimed to dissociate between these two phenomena. We induced senescence in HCT 116 cells by pulse treatment with doxorubicin and observed transiently increased ploidy, abnormal nuclear morphology, and various distributions of some proteins (e.g., p21, Ki-67, SA-β-galactosidase) in the subnuclei. Doxorubicin-treated HCT 116 cells displayed an increased production of reactive oxygen species (ROS) possibly caused by an increased amount of mitochondria, which are characterized by low membrane potential. A decrease in the level of ROS by Trolox partially protected the cells from polyploidization but not from senescence. Interestingly, a decreased level of ROS prevented the cells from escaping senescence. We also show that MCF7 cells senesce, but this is not accompanied by the increase of ploidy upon doxorubicin treatment. Moreover, they were stably growth arrested, thus proving that polyploidy but not senescence *per se* enables to regain the ability to proliferate. Our preliminary results indicate that the different propensity of the HCT 116 and MCF7 cells to increase ploidy upon cell senescence could be caused by a different level of the mTOR and/or Pim-1 kinases.

Neoplasia (2015) 17, 882–893

Introduction

Cell senescence is associated with irreversible growth arrest. Primary cells undergo senescence due to telomere erosion, which is known as replicative senescence [1], or due to stress or oncogenes, resulting in stress-induced premature senescence (SIPS), which is generally telomere erosion independent [2]. SIPS occurs in culture much faster than replicative senescence. Senescent cells despite being metabolically active have a changed metabolism in comparison with young cells. They secrete many factors, including proinflammatory ones, which give rise to the so-called senescence-associated secretory phenotype. Many other features are common for both replicative senescence and SIPS. The most frequently revealed ones are cell cycle arrest in the G1 or G2 phase of the cell cycle, increased size and granularity, activation of the DNA damage response, and increased activity of the so-called senescence-associated β-galactosidase (SA-β-Gal) [3,4].

Cancer cells avoid senescence and become immortal. However, recently, a plethora of reports documented that SIPS could be induced in cancer cells [5,6]. As a matter of fact, cellular senescence is considered to be an outcome of radio/chemotherapy. However, there is a growing body of evidence documenting that senescence of cancer

Address all correspondence to: Ewa Sikora, Laboratory of Molecular Bases of Aging, Nencki Institute of Experimental Biology, Polish Academy of Sciences, Warsaw, 02-093 Poland.
E-mail: g.mosieniak@nencki.gov.pl

[1] This work was supported by the Ministry of Science and Higher Education (grant N301 008 32/0549 and grant IP2012 062172), the National Center of Science (grant 2011/01/M/NZ1/01597), and the Foundation for Polish Science co-financed by the European Union under the European Social Fund (grant 125/UD/SKILLS/2013).
[2] These authors contributed equally to this work
Received 18 September 2015; Revised 11 November 2015; Accepted 16 November 2015

1476-5586
http://dx.doi.org/10.1016/j.neo.2015.11.008

cells can lead to cancer regrowth and may be the main cause of cancer cell repopulation observed in patients subjected to radio/chemotherapy [6]. We postulate that cancer cells' escape from senescence is strictly connected with cell polyploidization. Polyploidy is the result of endoreplication, which is endocycling and endomitosis. Endocycling cells pass DNA synthesis without mitosis. On the contrary, cells undergoing endomitosis execute an abortive mitosis that does not result in cell division, followed by subsequent reentering into the S phase. Both types of endoreplication can occur in cancer cells [7]. Recently, it was proposed that tumor cells containing an elevated genomic content are key players in the evolution of cancer [8].

Regrettably, in some reports showing cells escaping senescence, the issue of polyploidy was not addressed [9]. In other experiments which focused on polyploidy formation leading to cell divisions, cell senescence was not analyzed [10,11]. To our knowledge, there are only a few convincing studies showing the crucial role of polyploidy in cancer cell escape from senescence [12–17]. We also showed that polyploid cells en route to senescence were able to divide, giving rise to progeny having a different set of chromosomes than mother cells [18].

We asked the question whether reactive oxygen species (ROS) production can play a role in polyploidization/senescence of cancer cells. It was shown by others that the antioxidant *N*-acetyl-L-cysteine selectively eliminated polyploidy of prostate cancer cells, however, in these experiments, cell senescence was not considered [19]. In this study, we were able to show that an antioxidant Trolox can reverse, at least partially, polyploidy formation and inhibit clonogenicity but not senescence of doxorubicin-treated HCT 116 cells.

Doxorubicin (dox) is both a DNA damage and ROS-producing agent [20] as well as a potent antineoplastic drug used in the treatment of a variety of cancers [21]. DNA damage, including that evoked by ROS, is considered to be the main culprit of cell senescence [22], and it is a common effect of cancer cell radio/chemotherapy [23].

Materials and Methods

Cell Lines

The human colon HCT 116 cancer cell line was kindly provided by Dr. Bert Vogelstein (Johns Hopkins University, Baltimore, MD). The MCF7 cell line was obtained from ATCC. Authentication of both cell lines was performed this year by Cell Line Authentication IdentiCell STR using STR profiling.

Cells were grown under standard conditions (37°C, 5% CO_2) in McCoy's (HCT 116) or Dulbecco's modified Eagle's medium (MCF7) medium.

Senescence-Associated β-Galactosidase

SA-β-Gal was detected according to Dimri et al. [24] or by flow cytometry as previously described [18].

Cell Morphology Visualized by Hematoxylin Staining

Cells were fixed for 15 minutes in 96% ethanol at RT then washed with water and stained with 0.4% hematoxylin for 3 minutes.

Scanning Electron Microscopy

Samples were prepared according to Perletti et al. [25]. All specimens were observed under a microscope (Zeiss LEO 1430VP).

F-Actin Staining

Cells were fixed in 4% paraformaldehyde for 15 minutes on ice, washed in PBS, permeabilized with 0.1% Triton X-100 in PBS for 45 minutes, and incubated for 30 minutes with TRITC-labeled phalloidin diluted 1:1000 in PBS. DNA was stained with DAPI (1 μg/ml in PBS) for 15 minutes, washed again with PBS, and mounted with the mounting medium.

Immunocytochemistry

Cells grown on coverslips were fixed in ice-cold methanol for lamin A/C, p53 and p21 staining or in 4% paraformaldehyde (Sigma Aldrich, Poznan, Poland) at 4°C for 15 minutes for Aurora B and Ki-67 staining (Abcam, Cambridge, UK) or in ice-cold 70% ethanol for p-ATM (Ser1981) staining. Afterwards, cells were incubated on slides with the appropriate antibody, namely, anti-lamin A/C, anti-p53, and anti-p21(1:100) (Santa Cruz Biotechnology, Inc., Dallas, TX) anti-Aurora B (Becton Dickinson, Diag-med, Warsaw, Poland), anti-Ki-67 (1:200) (Abcam, Cambridge, UK), and anti-p-ATM (Ser1981) (1:900) (Millipore, Merck, Warsaw, Poland). Next, secondary Alexa 488– or Alexa Fluor 555–conjugated IgG antibody (1:1000) was used (Life Technology, Warsaw, Poland). To visualize the nuclei, DNA was stained using either DAPI (1 μg/ml in PBS) or DRAQ 5 (10 μM in PBS) (Life Technology, Warsaw, Poland). The specimens were analyzed using a fluorescent Nikon Eclipse 50i microscope with an EvolutionVF camera (MediaCybernetics) and the ImagePro Plus software or using a confocal microscope (described in the next section).

Alternatively, for Ki-67 visualization, the biotin-avidin detection system (Vectastain ABC Kit) was used as described previously [18]. The specimens were analyzed using Nikon Eclipse 50i microscope with an EvolutionVF camera (MediaCybernetics) and the ImagePro Plus software.

In the case of immunocytochemistry combined with SA-β-Gal staining, cells were firstly stained according to the foregoing protocol (detection of SA-β-Gal), washed twice with PBS, and stained as described above (without the fixation step).

Confocal Imaging

Specimens were visualized with confocal laser scanning microscope Leica TCS SP8 using a 63×/1.4 oil immersion lens. Fluorescence was excited using the 405-nm line from a pulsed laser (for Hoechst/DAPI) and white light laser for other fluorochromes. Emitted light was captured using a hybrid Leica detector. Confocal *z* section stacks were collected at 0.39-μm spacing through the depth of the specimen. The final images represent a maximum projection along the *z* axis.

ROS Measurement

Live cells were incubated with DCF-DA (20 μM in PBS) (Life Technologies,Warsaw, Poland) for 20 minutes in 37°C and then trypsinized and measured using the flow cytometry; 30,000 events were collected per sample.

Mitochondrial Mass Measurement

Live cells were incubated with MitoTracker Green FM (200 nM) (Life Technology, Warsaw, Poland) for 15 minutes at 37°C in a cell incubator, washed with PBS, and immediately measured using the flow cytometer. Results are presented as % of control mean fluorescence in FL1 channel.

Alternatively, cells on coverslips were incubated with MitoTracker Green FM, fixed in 4% paraformaldehyde mounted with mounting medium, and analyzed using a fluorescent Nikon Eclipse 50i microscope, CCD Evolutions VF camera (MediaCybernetics), and

the Image-Pro Plus 6.0 software or Leica DMI6000 with an HCX PL APO 63×/1.40-0.60 objective.

Mitochondrial Potential Measurement

Trypsynized cells were preincubated in standard medium for 25 minutes at 37°C and then incubated for 20 minutes with JC-9 (1 μg/ml) (Life Technology, Warsaw, Poland). Next, cells were washed with PBS and analyzed using the flow cytometer. Cells incubated with 1 μM FCCP (carbonyl cyanide 4-(trifluoromethoxy) phenylhydrazone) were used as a negative control.

DNA Content Analysis

For DNA analysis, cells were trypsinized, fixed in 70% ethanol, and stained with PI solution (3.8 mM sodium citrate, 50 mg/ml of RNAse A, 500 mg/ml of PI, in PBS). DNA content was determined using flow cytometry.

Western Blotting

Whole cell protein extracts were prepared according to the Laemmli method [26]. Equal amounts of protein were separated electrophoretically in 8%, 12%, or 15% SDS-polyacrylamide gels and afterwards transferred to nitrocellulose membranes. Membranes were probed with antibodies specific for p53 (DO-1, 1:500 in TBS with 5% milk), p21 (C-19, 1:500 in TBS/5% milk) (Santa Cruz Biotechnology, Inc., Dallas, TX), p-p53 (Ser15) (1:500 in TBS/5% BSA), PARP-1 (1:1000 in TBS/5% milk) (Becton Dickinson, Diag-med, Warsaw, Poland), β-catenin (1:2000 in TBS/5% BSA), p-p70S6K (Thr 389) (1:1000 in TBS/5% BSA), p70S6K (1:1000 in TBS/5% BSA), Pim-1(1:1000 in TBS/5% BSA) (Cell Signaling, Lab-JOT Ltd., Warsaw, Poland), and β-actin or GAPDH (1:30,000 in TBS/5% BSA) (Sigma Aldrich, Poznan, Poland) as a loading control. Proteins were detected using an appropriate secondary HRP-conjugated antibody (1:10,000 in TBS/5% milk) and ECL (GE Healthcare, Buckinghamshire, UK) reagents as recommended by the manufacturer.

Senescence-Associated Secretory Phenotype

Concentrations of the secreted proteins in the culture media were measured using a colorimetric enzyme-linked immunosorbent assay according to the protocol provided by the manufacturer (R&D, Biokom, Warsaw, Poland). The levels of cytokines (IL-8, VEGF) were determined with the use of standard curves, and the results were normalized to the total cell number.

Clonogenicity Assays

Cells were treated with dox for 24 hours and then cultured in a drug-free medium for the indicated time. Next, the cells were replated into 6-well plates at a density of 300 cells per well and cultured for additional 14 days. The colonies were fixed with methanol and stained with 4% methylene blue.

Flow Cytometry

All samples were analyzed using a FACS Calibur flow cytometer (Becton Dickinson, Warsaw, Poland) with CellQuest Software; 10,000 events were counted for each sample.

Results

Senescence Hallmarks of Doxorubicin-Treated HCT 116 Cells

Previously, we have shown that the HCT 116 cells treated with 100 nM dox for 1 day and then cultured in a drug-free medium for several days (1 + *n*) underwent senescence and became SA-β-Gal positive [18]. Now, we show their extended characteristic (Figure 1). We proved the formation of active ATM (p-ATM) foci (Figure 1*B*) and an increased level of the active form of p53 (phosphorylated on Ser 15, p-p53) (Figure 1*C*). ATM is a key enzyme in the DNA damage response signaling pathway which is upstream of p53/p21 [27]. Thus, we proved that the DNA damage response is activated in HCT 116 cells undergoing senescence. We only analyzed adherent cells which were not dying ones as PARP-1 cleavage could not be observed in these cells (Figure 1*C*). One of the important hallmarks of senescent cells is their ability to secrete a number of factors [28]. Accordingly, we observed an increased amount of IL-8 and VEGF in the medium of dox-treated cells (Figure 1*D*). Typical features of senescent cells are their increased size and granularity which were visualized by scanning electron microscopy and flow cytometry (Supp. 1, *A* and *B*). Hematoxylin staining revealed many perinuclear vacuoles. Some of them seemed to be connected with the nuclei (Supp. 1*C*).

Nuclear Morphology and Nuclear Protein Distribution in Doxorubicin-Treated HCT116 Cells

Dox-treated cells underwent intensive polyploidization. As revealed by the measurement of DNA content using flow cytometry, the subpopulation of cells having >4C DNA accounted for 50% of the entire population on days 1 + 4 and 1 + 5 [18]. DNA content analysis performed after a longer period of time revealed that the cells underwent subsequent depolyploidization (Figure 1*E*). Polyploidization and depoliploidization can be connected with the life cycle of cancer, and a different distribution of certain proteins in the subnuclei of the same polyploid cell has been shown [29,30]. Therefore, we were interested in how the nuclear morphology and protein expression connected with cell senescence (p21, SA-β-Gal) look like in polyploid cells induced to senesce.

Indeed, dox-treated cells seem to have a disorganized structure of the nuclear lamina as it is visible with lamin A/C staining (Figure 2*A*). As can be seen, in perinuclear vesicles, DNA is less stained, probably due to highly decondensed chromatin; however, nuclear proteins such as Aurora B, p53, and p21 are all localized in both the nuclei (colocalized with DNA) and perinuclear vesicles.

Figure 2, *A-D* shows nuclei of mononuclear cells; however, we have also observed many multinucleated cells. Interestingly, when we stained cells for p21, it appeared that, inside the same cell, both p21-positive and p21-negative micronuclei could be detected (Figure 2*E*).

Senescent cells are arrested in the G1 or G2 phase of the cell cycle. Ki-67 is frequently used as a negative marker of senescent, nonproliferating cells despite the fact that it was only shown that cells, which are in the G0 phase and are truly out of the cell cycle, are deprived of Ki-67 expression [31]. Thus, we double stained cells for Ki-67 and SA-β-Gal and observed cells under confocal microscope. The majority of dox-treated HCT 116 cells were Ki-67 positive (not shown). Moreover, we observed some cells which were double positive for Ki-67 and SA-β-Gal (Figure 3*A*), proving that they are not out of the cell cycle. However, we also observed cells which were negative for Ki-67 and positive for SA-β-Gal, thus implying that at least some senescent cells can escape the cell cycle. This issue needs further investigation.

We also showed that some cells were double stained for Ki-67 and p21 (Figure 3*B*).

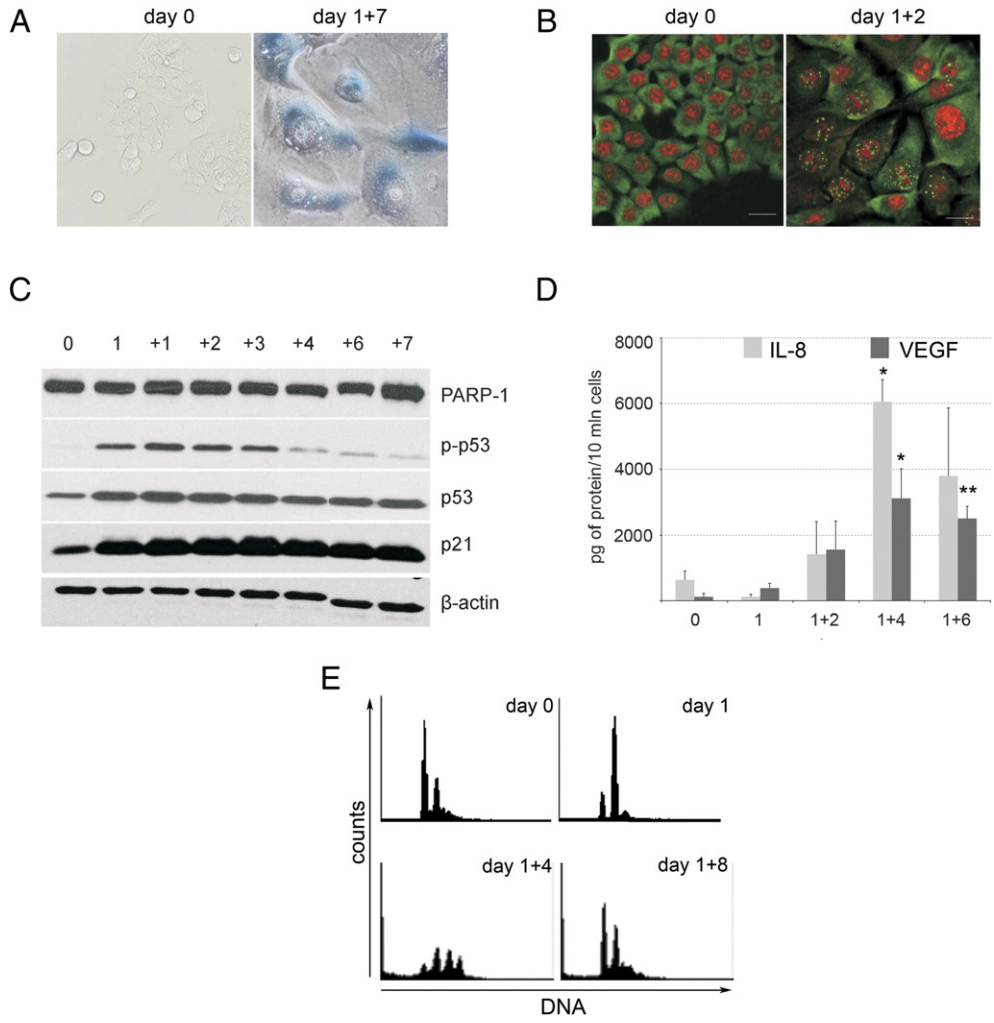

Figure 1. Markers of senescence in dox-treated HCT 116 cells. (A) SA-β-Gal–positive cells. Cells were untreated or dox treated for 1 + 7 days. Magnification is 200×. (B) Immunochemistry of p-ATM foci. Untreated cells and cells treated for 1 + 2 days are shown. Anti–p-ATM staining is shown in green; nuclei were visualized in red. The bar represents 30 μm. (C) Western blotting analysis of p-p53, p21, and PARP-1. β-Actin was used as a loading control. (D) The level of IL-8 and VEGF in the medium of dox-treated cells. Cells were treated as indicated, and the secretome was measured in five independent experiments. (E) DNA content measured by flow cytometry. Untreated (day 0) and dox-treated cells are shown as indicated. Statistical significance between untreated and dox-treated cells was estimated using the Student's *t* test. *$P < .05$, ** $P < .01$.

Altogether, our observations revealed abnormal morphology of the nuclei and different distribution of nuclear proteins inside the same cell, which could suggest different fate of the cells which arise after depolyploidization.

ROS Production in Doxorubicin-Treated HCT 116 Cells

Doxorubicin induced both DNA damage and ROS production. Subsequently, we analyzed the morphology and function of mitochondria, which could be the culprit of ROS production. Figure 4(*A,B*) shows some mitochondrial parameters in HCT 116 cells treated with dox. We used MitoTracker Green FM which preferentially accumulates in mitochondria, becomes fluorescent in their lipid environment, and thus gives an estimate of the mitochondrial mass in cells. We observed green fluorescence all over the cytoplasm; however, we found a dramatic increase in perinuclear MitoTracker Green fluorescence in giant cells (Figure 4*A*). This immunofluorescence data were confirmed using flow cytometry, showing again an increase in MitoTracker Green labeling in dox-treated cells already on day 1 that reached almost 300% on day 1 + 5 (Figure 4*B*, *left panel*). The increase in mitochondrial mass may result from the induction of a mitochondrial biogenesis program.

We used the cationic dye JC-9, which localizes to normal mitochondrial membranes in the form of red aggregates and turns into a green monomer upon membrane depolarization. Moreover, this dye indicates mitochondrial membrane potential independently of their mass which is important due to the fact that the mitochondrial mass is increased in giant senescent cells. The ratio of red/green mitochondria was calculated by flow cytometry, confirming that dox-treated cells show an increase in the proportion of depolarized mitochondria (Figure 4*B*, *right panel*). Because depolarized mitochondria can produce more ROS, we studied the level of H_2O_2 using a fluorescent probe, DCF-DA, and flow cytometry, and we observed its substantial increase on day 1 + 1 which was followed by a slight reduction on day 1 + 5 (Figure 4*B*, *lower panel*).

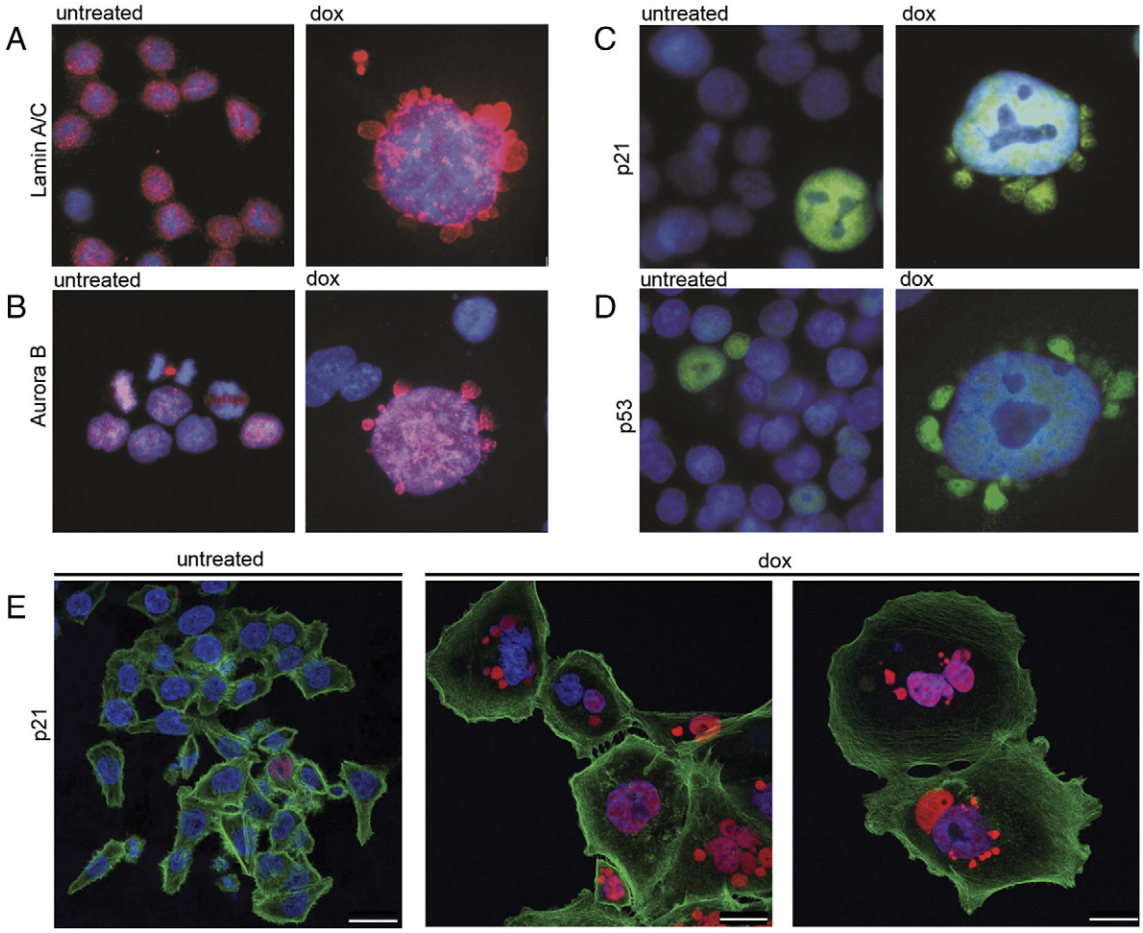

Figure 2. Perinuclear vesicles visualized by immunostaining of different nuclear proteins in untreated and dox-treated HCT 116 cells. Lamin A/C (A, red), Aurora B (B, red), p21 (C, green; E, red), and p53 (D, green). Nuclei were stained with DAPI (blue) and actin with phalloidin conjugated with TRITC (E, green). Cells are from day 1 + 5 (A-D) and day 1 + 3 (E). The cell gallery is presented. Each bar represents 25 μm.

Recently, the connection between β-catenin and ROS production was revealed during senescence of mesenchymal cells [32]. Indeed, we already observed an increased level of this protein on day 1 + 2, which persisted until the end of the experiment (Figure 4*C*).

As we documented an increased level of ROS in cells undergoing senescence, we were interested whether scavenging them can change the cell fate. Indeed, we observed a significant reduction of the level of ROS upon Trolox treatment (Figure 5*A*). Moreover, in the Trolox-treated population, there were fewer polyploid cells, but these were observed only on day 1 + 1 (Figure 5*B*). However, this treatment did not prevent the cells from undergoing senescence as it was revealed by SA-β-Gal activity measured using flow cytometry (Figure 5*C*). Interestingly, these cells had a substantially reduced colony formation capability, indicating that there were no senescence evaders and that ROS might be needed for the divisions of polyploid cells (Figure 5*D*).

Senescence, But Not Polyploidization, of Doxorubicin-Treated MCF7 Cells

We were interested whether other cells than HCT 116 can undergo dox-induced senescence which would not be connected with the polyploidization. Thus, we used the same protocol for the induction of senescence in MCF7 cells. As can be seen in Figure 6, these cells became SA-β-Gal positive (Figure 6*A*) and showed an increased level of p53, p-p53, and p21 (Figure 6*B*); however, their ploidy did not increase (they are already paratriploid) (Figure 6*C*). The clonogenicity assay displayed that their proliferation is stably arrested (Figure 6*D*). Moreover, we did not observe under the microscope the presence of small escapers (not shown). Thus, we can conclude that not senescence *per se* but increased ploidy is responsible for cell regrowth.

Different Expression of mTOR and Pim-1 in Dox-Treated HCT 116 and MCF-7 Cells

Subsequently, we asked the question whether some signaling molecules could be responsible for the different propensity of HCT 116 and MCF-7 cells to undergo polyploidization upon dox treatment. There are controversial data indicating the role of the p16/Rb signaling pathway in cancer cell senescence as well as in the escape from it (reviewed in [33]). However, our experiments excluded the possibility that pRb could be the possible factor responsible for the observed differences between the two cell lines (not shown). This could be explained by the fact that both types of cells lack the functional p16. Thus, we focused our attention on two serine/treonine kinases, namely, mTOR and Pim-1.

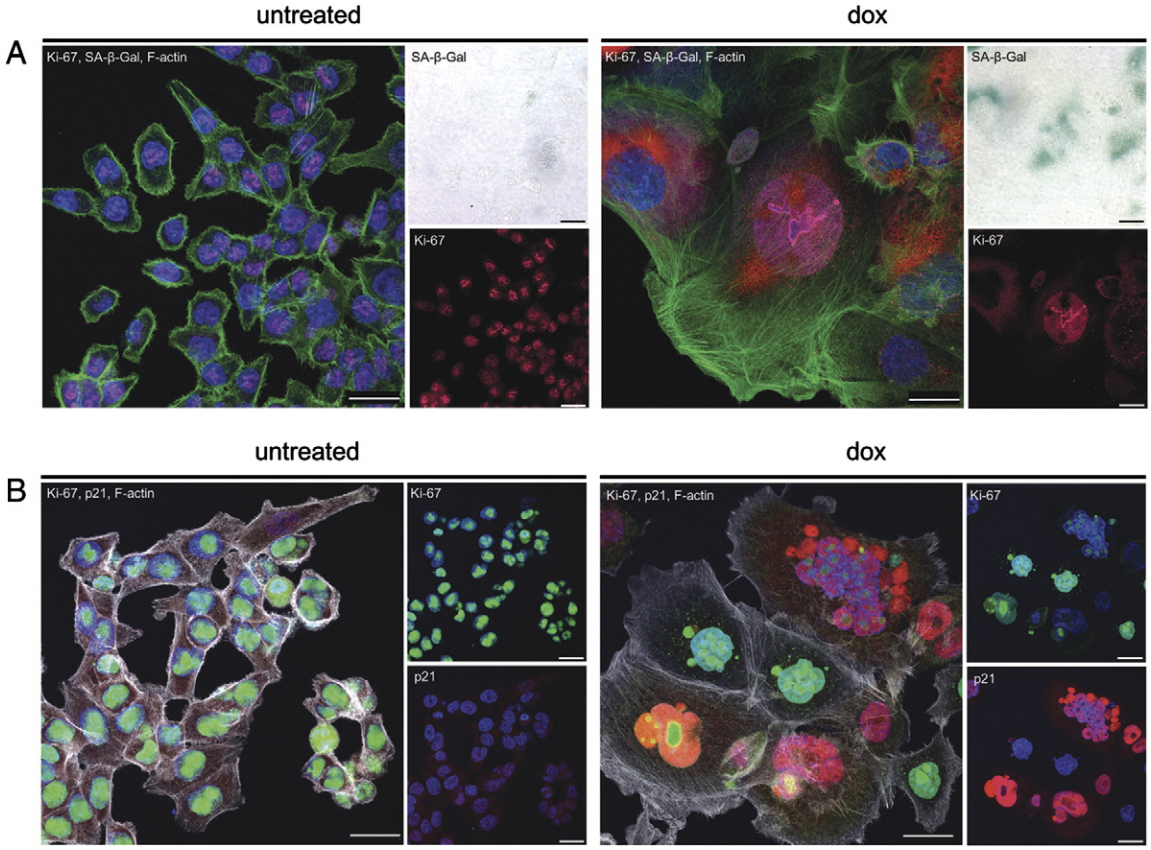

Figure 3. Nuclear protein staining (Ki-67 and p21) and SA-β-Gal activity in dox-treated HCT 116 cells. Cells were untreated or treated with dox (day 1 + 7) as indicated. (A) Cells triple stained for Ki-67 (pink), SA-β-Gal (red), and F-actin (white). SA-β-Gal is also shown in the light microscopy (upper right panel). (B) Cells triple stained for Ki-67 (green), p21 (red), and F-actin (white). Nuclei are blue (DAPI). Each bar represents 25 μM.

mTOR is essential for cell growth, protein translation, autophagy, and metabolism [34]. In numerous cancer types, the mTOR signaling pathway is activated by deregulation of its upstream factors, such as Akt activation, and stimulates cellular mass growth which is coupled with cell cycle progression. Furthermore, mTOR is associated with the development of cell polyploidization [35]. Recent studies have shown that mTOR inhibitors prevented the induction of polyploidy/senescence in breast cancer cells [36].

Our results (Figure 7*A*) have shown different activity of this kinase in dox-treated HCT 116 (increased) and MCF7 (not changed) cells, suggesting that its activation is rather connected with polyploidization (mass growth) than cell senescence.

The Pim-1 oncogene is the founding member of the Pim serine-threonine kinase family involved in the development of various tumors of hematological and epithelial origin [37]. It was demonstrated that overexpression of Pim-1 in human prostate and breast epithelial cells results in the gradual emergence of polyploid cells and that polyploidy induced by Pim-1 can promote the development of chromosomal abnormalities and tumorigenicity in human prostate and mammary epithelial cells [38]. Recently, it has been documented that Pim-1 is overexpressed during replicative and oncogene-induced senescence of normal human fibroblasts [39]. Others have shown that Pim-1 kinases prevent premature cardiac aging and are responsible for maintaining a healthy pool of functional mitochondria leading to efficient cellular energetics [40]. Our results show that MCF7 cells, in contrast to HCT116 cells, do not express Pim-1, which could explain the lack of increase in ploidy in these cells (Figure 7*B*). Furthermore, we observed a high basal level of Pim-1 in HCT 116 cells which transiently dropped. Surprisingly, this reduction seems to be associated with increased ploidy. These results indicate that indeed Pim-1 or other family members could be responsible for the different propensity of HCT 116 and MCF7 cells to undergo polyploidization upon dox treatment. This issue requires further investigation.

Discussion

Senescence of cancer cells is considered as an outcome of radio/chemotheraphy, and SA-β-Gal–positive cells were shown not only *in vitro* but also *in vivo* in tumor sections after therapy [6]. However, therapy-induced senescence seems not to be beneficial as it may lead to cancer recurrence.

Genomic instability, including polyploidy, is a characteristic feature of most cancers [41]. HCT 116 cells are not polyploid, but they have a near diploid set of chromosomes (70% of cells have 45 chromosomes). However, the pulse treatment of HCT116 cells with dox or curcumin leads to the formation of polyploid cells with the DNA increase reaching as much as 32C [18,42].

Subsequently, we observed gradual depolyploidization without the symptoms of cell death. The small cells outgrew the culture quite rapidly. The colonies of small cells were usually visible in the vicinity of giant cells.

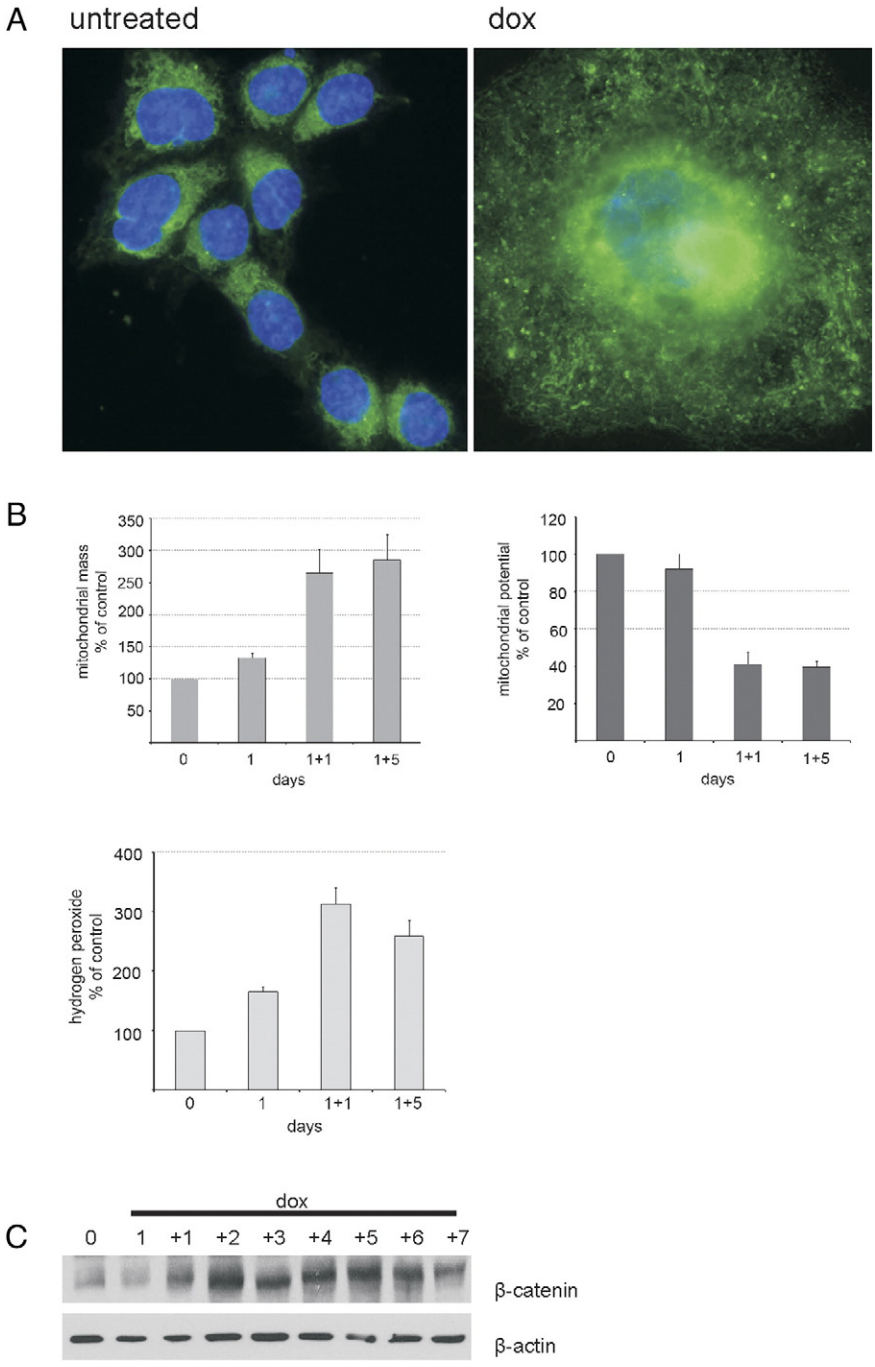

Figure 4. ROS production during senescence of HCT 116 cells. (A and B) Mitochondrial parameters in HCT 116 cells undergoing senescence. Visualization of mitochondria and mitochondrial mass was achieved using the MitoTracker Green FM and fluorescent microscope or flow cytometry, respectively. Mitochondrial potential and ROS level were measured using flow cytometry as described in Materials and Methods. The results are means from three independent experiments. Magnification is 600×. (C) β-Catenin in dox-treated cells as revealed by Western blotting.

Rajamaran and colleagues in their seminal work showed that polyploid cancer cells could divide by budding and produce, presumably, cancer stem cells, thus paving the way for understanding cancer cell repopulation after therapy [43]. Subsequently, Erenpreisa's group documented the presence of meiotic proteins during reversible polyploidy arguing for reductional divisions of polyploid cells, which can be followed by mitotic divisions of the descendants [44]. Recently, Zhang and colleagues documented that giant/polyploid but SA-β-Gal–negative cells can divide by budding and bursting, giving rise to the generation of cancer stem cells [45]. Our results further support the concept of amitotic division of polyploid cells. This type of division can be favored by labile nuclear lamina, as we have documented. We observed many perinuclear vesicles in giant cells. However, we could not detect DNA in these vesicles. Similar results were recently obtained in immortalized cells in which polyploidy and senescence were induced by irradiation [12]. In addition, others have shown vesicles in dox-treated HCT 116 cells containing DNA [13]. It cannot be excluded that they just contain a lower, hardly detectable

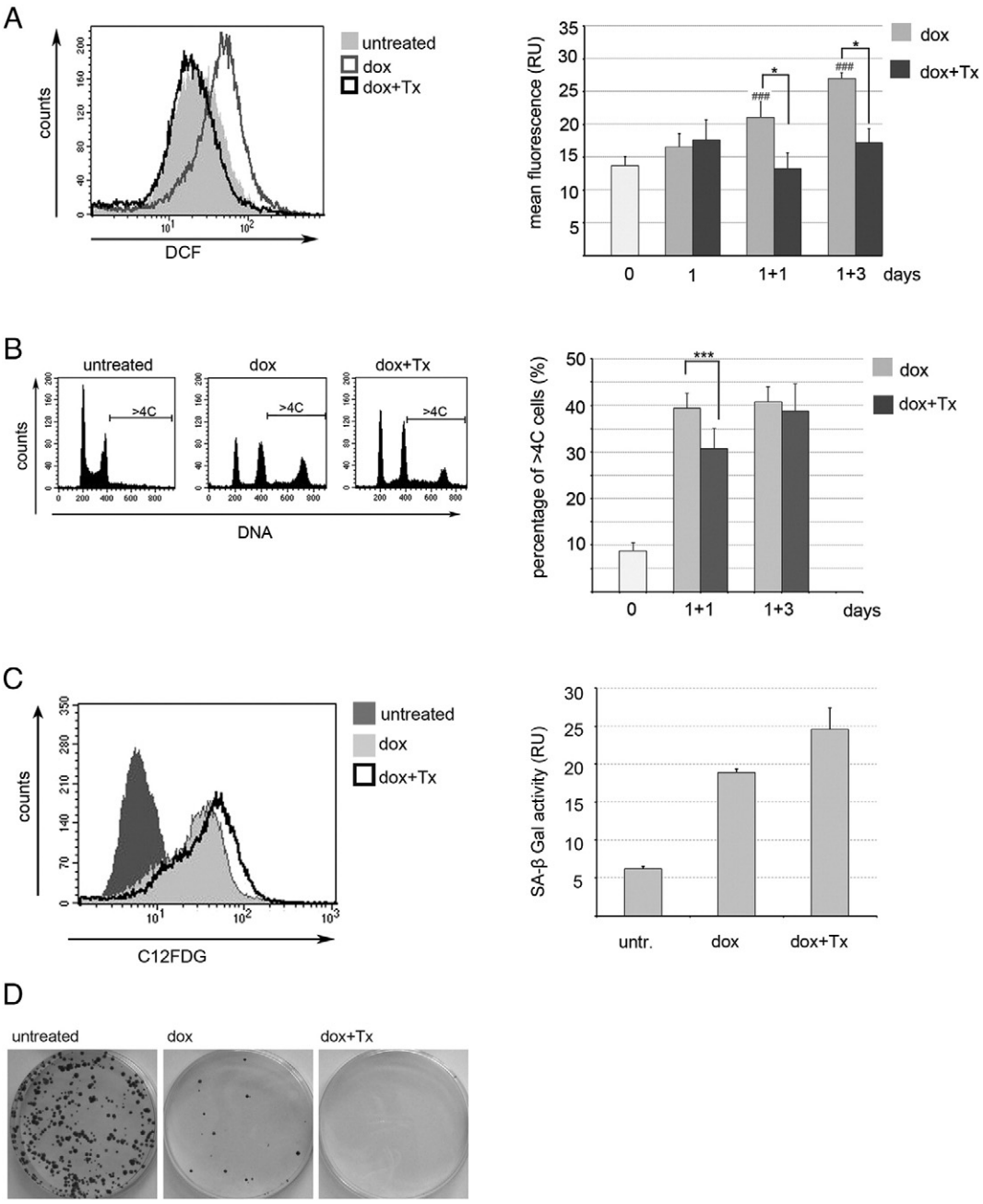

Figure 5. Trolox (Tx) reduced ROS production, polyploidy, and colony formation but not SA-β-Gal activity in dox-treated HCT116 cells. (A, left panel) Analysis of the level of ROS (DCF fluorescence) in untreated, dox-treated, and dox + Tx–treated cells on day 1 + 1. Representative histogram of flow cytometric measurement. (Right panel) A compilation of the ROS level analysis from five independent experiments. Statistical significance between untreated and dox-treated cells (###$P < .001$) as well as dox-treated and dox + Tx–treated cells (*$P < .05$) was estimated using the Student's *t* test. (B, left panel) Representative histograms of DNA content analysis (day 1 + 1). (Right panel) A compilation of the level of polyploidy in untreated, dox-treated, and dox + Tx–treated cells on indicated days (four independent experiments). Statistical significance was analyzed using the Student's *t* test. *** $P < .001$. (C, left panel) A representative histogram of flow cytometric analysis of SA-β-Gal activity in untreated, dox-treated, and dox + Tx–treated cells on day 1 + 3. C12FDG is a SA-β-Gal substrate. (D) A representative image of the colony formation assay of cells either untreated or treated with dox or dox + Tx (day 1 + 5).

amount of chromatin. We showed that many of DAPI-stained entities observed within the giant cells were also Ki67 positive. Thus, no one can deny the existence of heterogeneity in the mode of division of these genetically unstable cells. Although we believe that polyploidy is followed by amitotic divisions of polyploid cells, no one can also exclude other possibilities. We observed a lot of multinucleated cells with different DNA content suggesting that they could have underwent aberrant mitoses. Although some SA-β-Gal–positive cells are Ki-67 negative, the majority of giant cells preserve the capacity to divide. Others have shown that SA-β-Gal–positive cells simultaneously express Ki-67 and occasionally divide. This "SWING" is dependent on p21 and telomerase

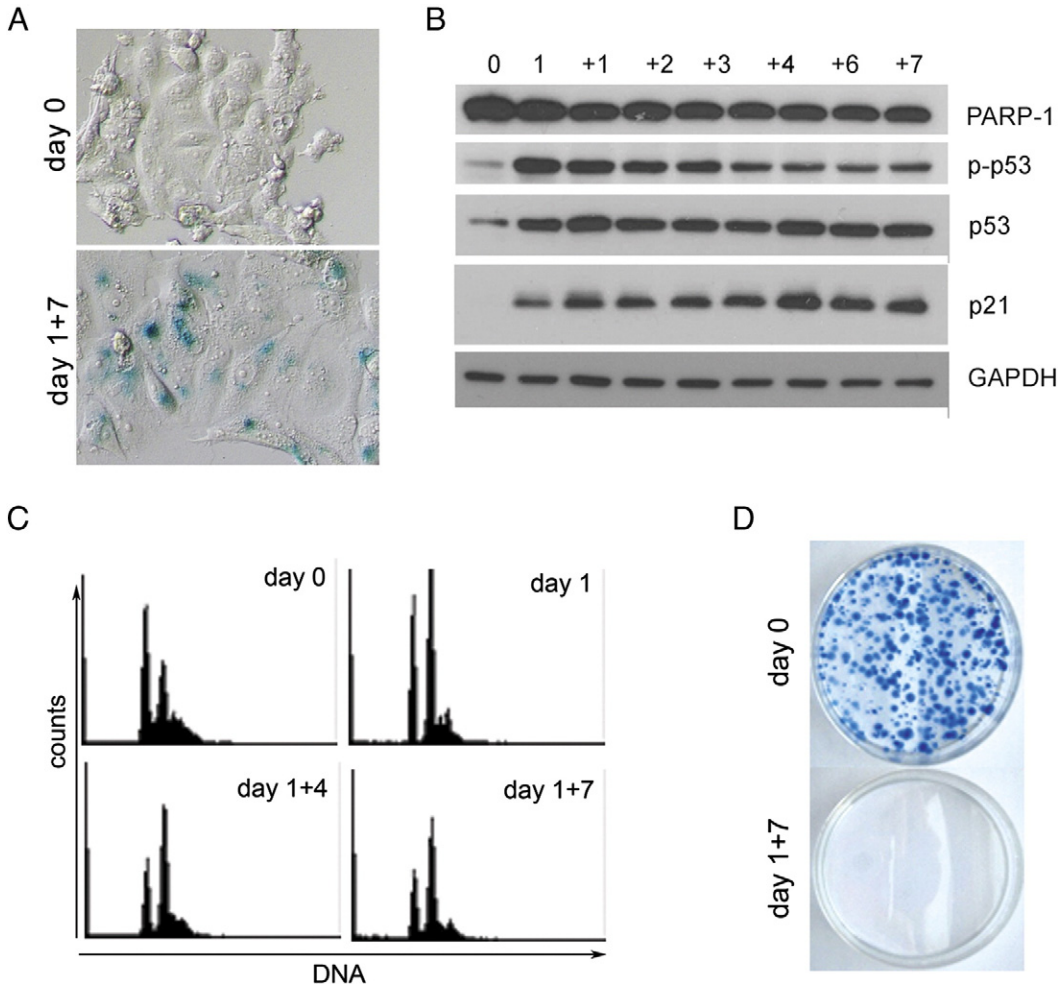

Figure 6. Markers of senescence of dox-treated MCF-7 cells. (A) SA-β-Gal–positive cells. Cells were untreated (day 0) or dox treated until day 1 + 7. (B) Western blotting analysis of p53, p-p53, p21, and PARP-1. (C) DNA content measured using flow cytometer. Days of treatment are indicated. (D) A representative image of the colony formation assay of cells either untreated or treated with dox (day 1 + 7).

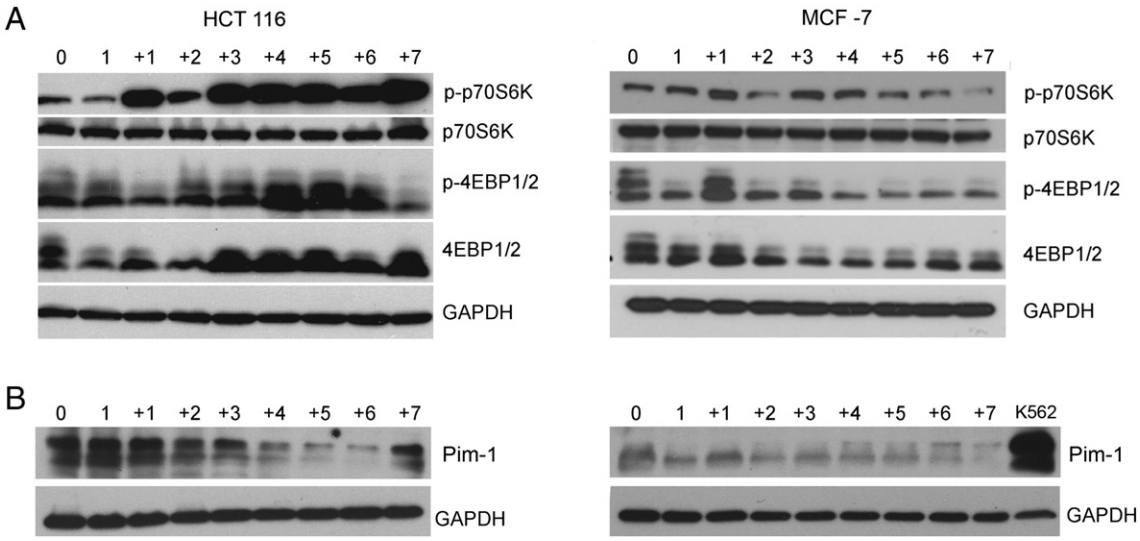

Figure 7. mTOR and Pim-1 level in dox-treated HCT 116 and MCF7 cells. (A) Western blotting analysis of the mTOR substrates p70S6 and 4EBP1/2 and their phosphorylated forms. (B) Pim-1 level. K562 cells were used as a positive control for Pim-1 expression. GAPDH was used as a loading control.

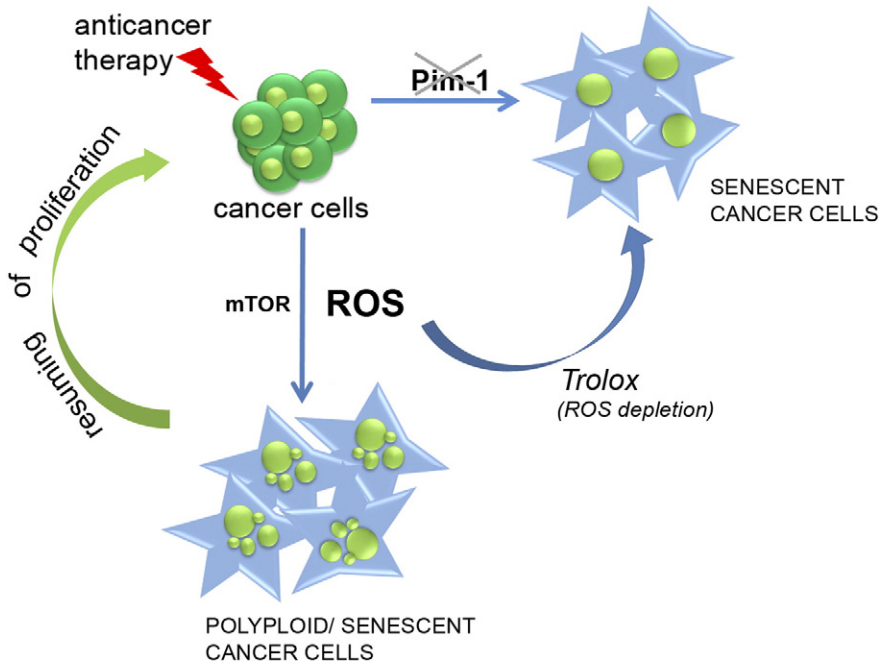

Figure 8. Scheme outlining the role of polyploidy formation, ROS scavenging, as well as mTOR activity and Pim-1 level in reversed and unreversed senescence of cancer cells. Cancer cells treated with anticancer agent undergo either senescence or polyploidization/senescence. Polyploidization is associated with the increase of ROS level and the resuming of cell divisions, which can be avoided by antioxidant treatment. Basal Pim-1 expression and mTOR activation seem to be indispensable for polyploidy formation.

competency [46]. Similarly, Jackson et al. [30] showed that both p21 and OCT-4 could be expressed in the same cell. On the contrary, others provided evidence that only escapers of drug-induced senescence had a tumor stem cell–like phenotype [9,12]. Because, in MCF7 cells, which do not increase polyploidization upon dox treatment, we did not observe cells which were able to escape senescence, we speculate that the formation of polyploidy is indispensable for abnormal divisions and escaping senescence. Interestingly, others have reported the evasion of progeny in dox-treated MCF7 cells; however, the involvement of polyploidy was not considered in that study [47]. The molecular mechanism showing polyploidy formation is still awaiting elucidation.

Some explanation of this phenomenon can come from revealing the role of ROS in senescent cells and in the evaders. Gosselin and colleagues documented that oxidative stress induced epithelial cell senescence and that these cells were able to divide by "budding-mitosis" [48]. This is in favor of our results showing that doxorubicin treatment generates ROS production and mitochondrial changes in giant cells and scavenging ROS by Trolox protected from the emergence of escapers. Similarly, Achuthan and colleagues documented that a senescent population of cancer cells had a high level of ROS. Moreover, they occasionally generated stem-like cells with low ROS [9].

It has been postulated, at least for replicative cell senescence, that ROS production is necessary for the stability of growth arrest during the establishment of the senescent phenotype [49]. On the contrary, Blagosklonny postulated that the main drawing force for senescence is mTOR, which induces hyperfunction including ROS production [50]. We show that ROS scavenging did not protect from dox-induced senescence, but the number of polyploid cells was slightly and temporarily diminished after Trolox treatment. Moreover, Trolox protected from the emergence of small escapers, which could be the progeny of giant polyploid ones. However, we cannot definitely exclude the role of ROS in cell senescence as we only measured the level of ROS till day 1 + 3 and their increase might occur at later time points when they might participate in establishing the senescence phenotype. Accordingly, we speculate that the subtle balance of the level of ROS can be responsible for their growth arrest/stimulation capability.

We also decided to investigate whether the differences in the expression of two kinases (mTOR and Pim-1) in these cells could be responsible for their propensity to form polyploid cells. mTOR might be connected with cell senescence by different mechanisms. One is the so-called geroconversion, which is postulated by Blagosklonny [51], and the second one is autophagy [52]. As the role of both processes in cell senescence is rather controversial and unlikely to be helpful in explaining the reversibility of cell senescence, our interpretation of the different activity of mTOR in HCT 116 and MCF7 cells focused on its possible role in polyploidy formation. Indeed, it seems that there is an increased activity of this kinase only in polyploidizing HCT 116 cells. Our other candidate, Pim-1, looks very promising, although its role in cell senescence seems to depend very much on the cell type. Nonetheless, our feeling is that the issue of the role of Pim-1 in polyploidy/senescence deserves further elucidation.

The main conclusion which emerges from our studies is that drug treatment of cancer cells can lead to their senescence; however, the cells which along with senescence undergo polyploidization are prone to escape this process. ROS scavengers prevent polyploidy formation and evasion of senescence. Thus, the increase of ploidy, not senescence *per se*, favors emergence of the progeny. Cells which are not immanently able to undergo polyploidization upon senescence-inducing conditions are protected from reversible senescence. The high basal level of Pim-1 and increased activity of mTOR after cell treatment seem to be indispensable for the association with

senescence ploidy formation. This idea is outlined in the scheme presented in Figure 8.

Our results might contribute to the development of anticancer therapy through protection of senescence-induced polyploidization.

Acknowledgement

This work was supported by the Ministry of Science and Higher Education (grant N301 008 32/0549 and grant IP2012 062172), the National Center of Science (grant 2011/01/M/NZ1/01597), and the Foundation for Polish Science co-financed by the European Union under the European Social Fund (grant 125/UD/SKILLS/2013). Nencki Institute is a beneficiary of the EU FP7 Project BIO-IMAGINE: BIO-IMAGing in research INnovation and Education, GA No. 264173.

Appendix A. Supplementary data

Supplementary data to this article can be found online at http://dx.doi.org/10.1016/j.neo.2015.11.008.

References

[1] Hayflick L and Moorhead PS (1961). The serial cultivation of human diploid cell strains. *Exp Cell Res* **25**, 585–621.
[2] Kuilman T, Michaloglou C, Mooi WJ, and Peeper DS (2010). The essence of senescence. *Genes Dev* **24**(22), 2463–2479.
[3] Campisi J and d'Adda di Fagagna F (2007). Cellular senescence: when bad things happen to good cells. *Nat Rev Mol Cell Biol* **8**(9), 729–740.
[4] Sikora E, Arendt T, Bennett M, and Narita M (2011). Impact of cellular senescence signature on ageing research. *Ageing Res Rev* **10**(1), 146–152.
[5] Roninson IB, Broude EV, and Chang BD (2001). If not apoptosis, then what? Treatment-induced senescence and mitotic catastrophe in tumor cells. *Drug Resist Updat* **4**(5), 303–313.
[6] Wu PC, Wang Q, Grobman L, Chu E, and Wu DY (2012). Accelerated cellular senescence in solid tumor therapy. *Exp Oncol* **34**(3), 298–305.
[7] Fox DT and Duronio RJ (2013). Endoreplication and polyploidy: insights into development and disease. *Development* **140**(1), 3–12.
[8] Coward J and Harding A (2014). Size does matter: why polyploid tumor cells are critical drug targets in the war on cancer. *Front Oncol* **4**, 123.
[9] Achuthan S, Santhoshkumar TR, Prabhakar J, Nair SA, and Pillai MR (2011). Drug-induced senescence generates chemoresistant stemlike cells with low reactive oxygen species. *J Biol Chem* **286**, 37813–37829.
[10] Zhang S, Mercado-Uribe I, and Liu J (2014). Tumor stroma and differentiated cancer cells can be originated directly from polyploid giant cancer cells induced by paclitaxel. *Int J Cancer* **134**(3), 508–518.
[11] Zhang S, Mercado-Uribe I, Xing Z, Sun B, Kuang J, and Liu J (2014). Generation of cancer stem-like cells through the formation of polyploid giant cancer cells. *Oncogene* **33**, 116–128.
[12] Chitikova ZV, Gordeev SA, Bykova TV, Zubova SG, Pospelov VA, and Pospelova TV (2014). Sustained activation of DNA damage response in irradiated apoptosis-resistant cells induces reversible senescence associated with mTOR downregulation and expression of stem cell markers. *Cell Cycle* **13**, 1424–1439 [United States].
[13] Mansilla S, Bataller M, and Portugal J (2009). A nuclear budding mechanism in transiently arrested cells generates drug-sensitive and drug-resistant cells. *Biochem Pharmacol* **78**, 123–132.
[14] Puig PE, Guilly MN, Bouchot A, Droin N, Cathelin D, Bouyer F, Favier L, Ghiringhelli F, Kroemer G, and Solary E, et al (2008). Tumor cells can escape DNA-damaging cisplatin through DNA endoreduplication and reversible polyploidy. *Cell Biol Int* **32**(9).
[15] Sabisz M and Skladanowski A (2009). Cancer stem cells and escape from drug-induced premature senescence in human lung tumor cells: implications for drug resistance and in vitro drug screening models. *Cell Cycle* **8**(19), 3208–3217.
[16] Wang Q, Wu PC, Dong DZ, Ivanova I, Chu E, Zeliadt S, Vesselle H, and Wu DY (2013). Polyploidy road to therapy-induced cellular senescence and escape. *Int J Cancer* **132**(7), 1505–1515.
[17] Weihua Z, Lin Q, Ramoth AJ, Fan D, and Fidler IJ (2011). Formation of solid tumors by a single multinucleated cancer cell. *Cancer* **117**(17), 4092–4099.
[18] Sliwinska MA, Mosieniak G, Wolanin K, Babik A, Piwocka K, Magalska A, Szczepanowska J, Fronk J, and Sikora E (2009). Induction of senescence with doxorubicin leads to increased genomic instability of HCT116 cells. *Mech Ageing Dev* **130**(1–2), 24–32.
[19] Roh M, van der Meer R, and Abdulkadir SA (2012). Tumorigenic polyploid cells contain elevated ROS and ARE selectively targeted by antioxidant treatment. *J Cell Physiol* **227**(2), 801–812.
[20] Gewirtz DA (1999). A critical evaluation of the mechanisms of action proposed for the antitumor effects of the anthracycline antibiotics adriamycin and daunorubicin. *Biochem Pharmacol* **57**(7), 727–741.
[21] Weiss RB (1992). The anthracyclines: will we ever find a better doxorubicin? *Semin Oncol* **19**(6), 670–686.
[22] d'Adda di Fagagna F (2008). Living on a break: cellular senescence as a DNA-damage response. *Nat Rev Cancer* **8**(7), 512–522.
[23] Lord CJ and Ashworth A (2012). The DNA damage response and cancer therapy. *Nature* **481**(7381), 287–294.
[24] Dimri GP, Lee X, Basile G, Acosta M, Scott G, Roskelley C, Medrano EE, Linskens M, Rubelj I, and Pereira-Smith O (1995). A biomarker that identifies senescent human cells in culture and in aging skin in vivo. *Proc Natl Acad Sci U S A* **92**(20), 9363–9367.
[25] Perletti G, Marras E, Dondi D, Osti D, Congiu T, Ferrarese R, de Eguileor M, and Tashjian Jr AH (2005). p21(Waf1/Cip1) and p53 are downstream effectors of protein kinase C delta in tumor suppression and differentiation in human colon cancer cells. *Int J Cancer* **113**(1), 42–53.
[26] Laemmli UK (1970). Cleavage of structural proteins during the assembly of the head of bacteriophage T4. *Nature* **227**(5259), 680–685.
[27] Bensimon A, Aebersold R, and Shiloh Y (2011). Beyond ATM: the protein kinase landscape of the DNA damage response. *FEBS Lett* **585**, 1625–1639 [Netherlands].
[28] Coppe JP, Desprez PY, Krtolica A, and Campisi J (2010). The senescence-associated secretory phenotype: the dark side of tumor suppression. *Annu Rev Pathol* **5**, 99–118.
[29] Erenpreisa J and Cragg MS (2007). Cancer: a matter of life cycle? *Cell Biol Int* **31**(12), 1507–1510.
[30] Jackson TR, Salmina K, Huna A, Inashkina I, Jankevics E, Riekstina U, Kalnina Z, Ivanov A, Townsend PA, and Cragg MS, et al (2013). DNA damage causes TP53-dependent coupling of self-renewal and senescence pathways in embryonal carcinoma cells. *Cell Cycle* **12**, 430–441.
[31] Scholzen T and Gerdes J (2000). The Ki-67 protein: from the known and the unknown. *J Cell Physiol* **182**(3), 311–322.
[32] Zhang DY, Pan Y, Zhang C, Yan BX, Yu SS, Wu DL, Shi MM, Shi K, Cai XX, and Zhou SS, et al (2012). Wnt/beta-catenin signaling induces the aging of mesenchymal stem cells through promoting the ROS production. *Mol Cell Biochem* **374**(1–2), 13–20.
[33] Chakradeo S, Elmore LW, and Gewirtz DA (2015). Is senescence reversible? Current drug targets; 2015.
[34] Meric-Bernstam F and Gonzalez-Angulo AM (2009). Targeting the mTOR signaling network for cancer therapy. *J Clin Oncol* **27**(13), 2278–2287.
[35] Ma D, Yu H, Lin D, Sun Y, Liu L, Liu Y, Dai B, Chen W, and Cao J (2009). S6K1 is involved in polyploidization through its phosphorylation at Thr421/Ser424. *J Cell Physiol* **219**(1), 31–44.
[36] Sharma S, Yao HP, Zhou YQ, Zhou J, Zhang R, and Wang MH (2014). Prevention of BMS-777607-induced polyploidy/senescence by mTOR inhibitor AZD8055 sensitizes breast cancer cells to cytotoxic chemotherapeutics. *Mol Oncol* **8**(3), 469–482.
[37] Nawijn MC, Alendar A, and Berns A (2011). For better or for worse: the role of Pim oncogenes in tumorigenesis. *Nat Rev Cancer* **11**(1), 23–34.
[38] Roh M, Franco OE, Hayward SW, van der Meer R, and Abdulkadir SA (2008). A role for polyploidy in the tumorigenicity of Pim-1–expressing human prostate and mammary epithelial cells. *PLoS One* **3**(7)e2572.
[39] Jin B, Wang Y, Wu CL, Liu KY, Chen H, and Mao ZB (2014). PIM-1 modulates cellular senescence and links IL-6 signaling to heterochromatin formation. *Aging Cell* **13**(5), 879–889.
[40] Mohsin S, Khan M, Nguyen J, Alkatib M, Siddiqi S, Hariharan N, Wallach K, Monsanto M, Gude N, and Dembitsky W, et al (2013). Rejuvenation of human cardiac progenitor cells with Pim-1 kinase. *Circ Res* **113**(10), 1169–1179.
[41] Negrini S, Gorgoulis VG, and Halazonetis TD (2010). Genomic instability—an evolving hallmark of cancer. *Nat Rev Mol Cell Biol* **11**(3), 220–228.
[42] Mosieniak G, Adamowicz M, Alster O, Jaskowiak H, Szczepankiewicz AA, Wilczynski GM, Ciechomska IA, and Sikora E (2012). Curcumin induces permanent growth arrest of human colon cancer cells: link between senescence and autophagy. *Mech Ageing Dev* **133**(6), 444–455.

[43] Sundaram M, Guernsey DL, Rajaraman MM, and Rajaraman R (2004). Neosis: a novel type of cell division in cancer. *Cancer Biol Ther* **3**(2), 207–218.
[44] Erenpreisa J and Cragg MS (2013). Three steps to the immortality of cancer cells: senescence, polyploidy and self-renewal. *Cancer Cell Int* **13**(1), 92.
[45] Fujioka S, Schmidt C, Sclabas GM, Li Z, Pelicano H, Peng B, Yao A, Niu J, Zhang W, and Evans DB, et al (2004). Stabilization of p53 is a novel mechanism for proapoptotic function of NF-kappaB. *J Biol Chem* **279**(26), 27549–27559.
[46] Sherman MY, Meng L, Stampfer M, Gabai VL, and Yaglom JA (2011). Oncogenes induce senescence with incomplete growth arrest and suppress the DNA damage response in immortalized cells. *Aging Cell* **10**(6), 949–961.
[47] Elmore LW, Di X, Dumur C, Holt SE, and Gewirtz DA (2005). Evasion of a single-step, chemotherapy-induced senescence in breast cancer cells: implications for treatment response. *Clin Cancer Res* **11**(7), 2637–2643.
[48] Gosselin K, Martien S, Pourtier A, Vercamer C, Ostoich P, Morat L, Sabatier L, Duprez L, de Roodenbeke C T'kint, and Gilson E, et al (2009). Senescence-associated oxidative DNA damage promotes the generation of neoplastic cells. *Cancer Res* **69**, 7917–7925.
[49] Passos JF, Nelson G, Wang C, Richter T, Simillion C, Proctor CJ, Miwa S, Olijslagers S, Hallinan J, and Wipat A, et al (2010). Feedback between p21 and reactive oxygen production is necessary for cell senescence. *Mol Syst Biol* **6**, 347.
[50] Blagosklonny MV (2008). Aging: ROS or TOR. *Cell Cycle* **7**(21), 3344–3354.
[51] Blagosklonny MV (2012). Cell cycle arrest is not yet senescence, which is not just cell cycle arrest: terminology for TOR-driven aging. *Aging (Albany NY)* **4**(3), 159–165.
[52] Gewirtz DA (2013). Autophagy and senescence: a partnership in search of definition. *Autophagy* **9**, 808–812.